Electronic Supplementary Material (ESI) for Analyst.


# Electronic Supplementary Information

## An N-linked disalicylaldehyde together with its caesium ion and dichloromethane sensing performances: 'Dual key & lock' LMCT-enhanced fluorescence strategy

Kun Zhang,* Ting-Ting Chen, Yin-Jing Shen, Zhuo-Ran Yang, Yan Huang, Shishen Zhang, Jiadan Xue and Benxia Li

Department of Chemistry, Zhejiang Sci-Tech University, Xiasha Higher Education District, Hangzhou 310018, P. R. China

### Tables

**Table S1** Crystal data and structural refinements for complexes $H_2Q_j$.

| Compound | $H_2Q_j$ |
|---|---|
| Empirical formula | $C_{23}H_{19}Cl_2NO_4$ |
| Formula weight | 444.29 |
| Temperature / K | 293(2) |
| Wavelength / Å | 0.71073 |
| Crystal Size (mm) | 0.27×0.32×0.36 |
| Crystal system | Triclinic |
| Space group | $P\bar{1}$ |
| $a$ / Å | 9.355(1) |
| $b$ / Å | 10.350(1) |
| $c$ / Å | 12.187(1) |
| $\alpha$ / ° | 65.857(2) |
| $\beta$ / ° | 87.964(3) |
| $\gamma$ / ° | 84.847(3) |
| $V$ / Å$^3$ | 1072.4(2) |
| $Z$ / $D_{calcd}$ (g / cm$^3$) | 2 / 1.376 |
| $F$(000) | 460 |
| $\mu$ / mm$^{-1}$ | 0.332 |
| $h_{min}$ / $h_{max}$ | –12 / 12 |
| $k_{min}$ / $k_{max}$ | –13 / 13 |
| $l_{min}$ / $l_{max}$ | –15 / 15 |
| Data / parameters | 4945 / 273 |
| $R_1$, w$R_2$ [$I > 2\sigma(I)$][a] | $R_1$ = 0.0795, w$R_2$ = 0.2243 |
| $R_1$, w$R_2$ (all data)[a] | $R_1$ = 0.1411, w$R_2$ = 0.2638 |
| $S$ | 1.03 |
| Max/min $\Delta\rho$/e Å$^{-3}$ | 0.81 / –0.55 |

[a] $R_1 = \Sigma||Fo|-|Fc|| / \Sigma|Fo|$, $wR_2 = [\Sigma[w(Fo^2-Fc^2)^2] / \Sigma w(Fo^2)^2]^{1/2}$

**Table S2** Selected bond distances (Å) and angles (°) in complexes $H_2Q_j$.

| Bond distances | | Bond angles | |
|---|---|---|---|
| $H_2Q_j$ | | | |
| Cl1–C4 | 1.743(5) | C8–N1–C17 | 111.3(3) |
| Cl2–C12 | 1.758(5) | C9–N1–C17 | 109.8(3) |
| O1–C1 | 1.192(6) | C8–N1–C9 | 109.2(3) |
| O2–C7 | 1.341(6) | O1–C1–C2 | 125.1(6) |
| O3–C15 | 1.301(5) | Cl1–C4–C5 | 118.9(3) |
| O4–C16 | 1.126(6) | Cl1–C4–C3 | 120.4(3) |
| N1–C8 | 1.471(5) | O2–C7–C6 | 120.5(3) |
| N1–C9 | 1.478(4) | O2–C7–C2 | 119.7(3) |
| N1–C17 | 1.473(5) | N1–C8–C6 | 111.5(3) |
| | | N1–C9–C10 | 113.0(3) |
| | | Cl2–C12–C13 | 120.6(4) |
| | | Cl2–C12–C11 | 119.5(4) |
| | | O3–C15–C14 | 121.2(4) |
| | | O3–C15–C10 | 118.5(4) |
| | | O4–C16–C14 | 125.8(5) |
| | | N1–C17–C18 | 113.2(3) |

Symmetry codes: [a], 2–*x*, –*y*, 1–*z*; [b], 1–*x*, 1–*y*, –*z*; [c], *x*, –*y*, *z*.

**Table S3** Hydrogen bonding parameters (Å, °) in macrocyclic complexes $H_2Q_j$.

| D–H···A | D–H | H···A | D···A | ∠DHA | Symmetry code |
|---|---|---|---|---|---|
| $H_2Q_j$ | | | | | |
| O2–H2···N1 | 0.82 | 1.92 | 2.648(4) | 148 | |
| O3–H3···O4 | 0.82 | 1.91 | 2.626(5) | 145 | |

## Figures

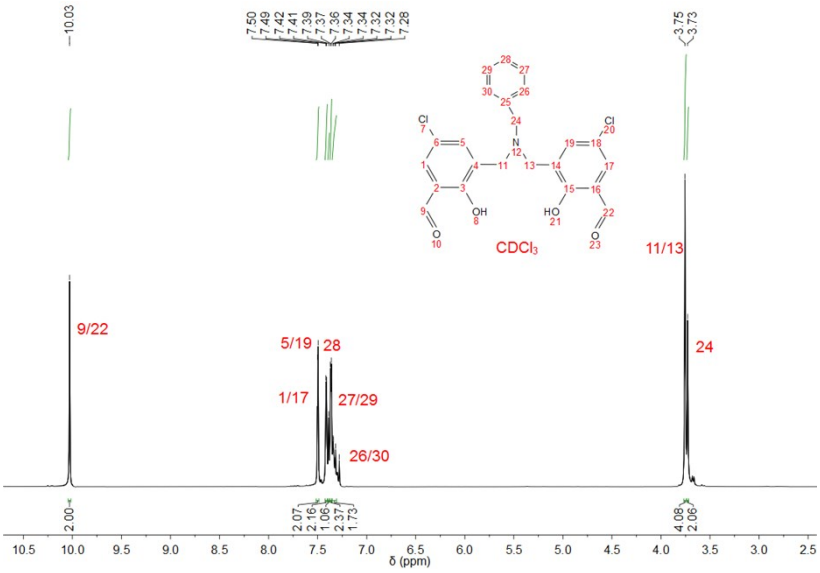


**Fig. S1** $^{1}$H NMR spectrum of dialdehyde $H_2Q_j$ in $CDCl_3$.

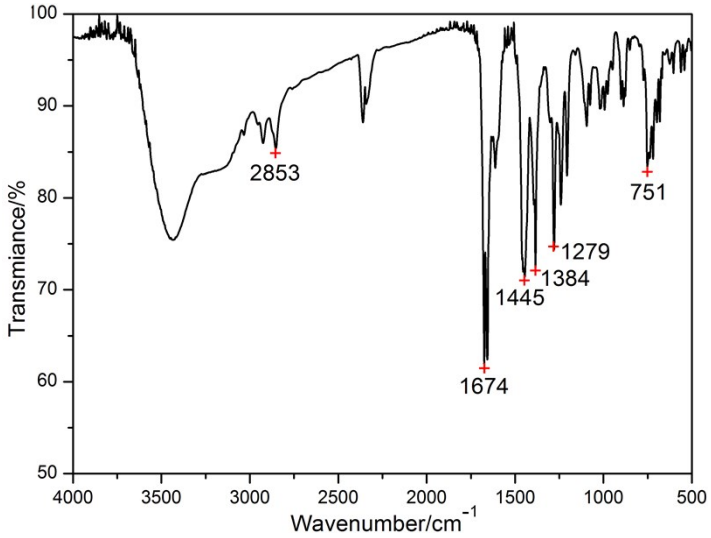


**Fig. S2** FT-IR spectrum of the dialdehyde compound $H_2Q_j$.

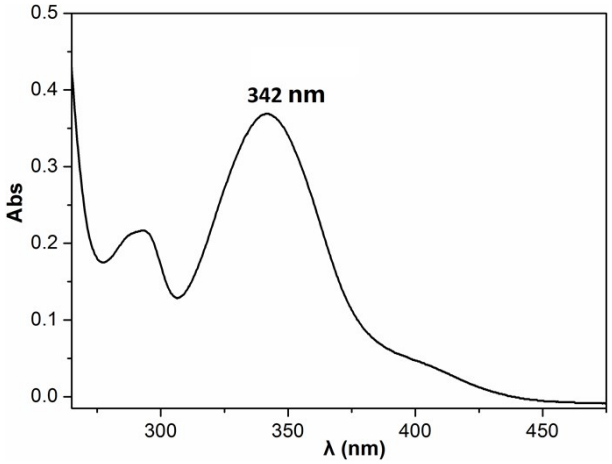


**Fig. S3** Absorption spectra of dialdehyde $H_2Q_j$ ([M] = 50 μM) in $CH_3OH$ at room temperature.

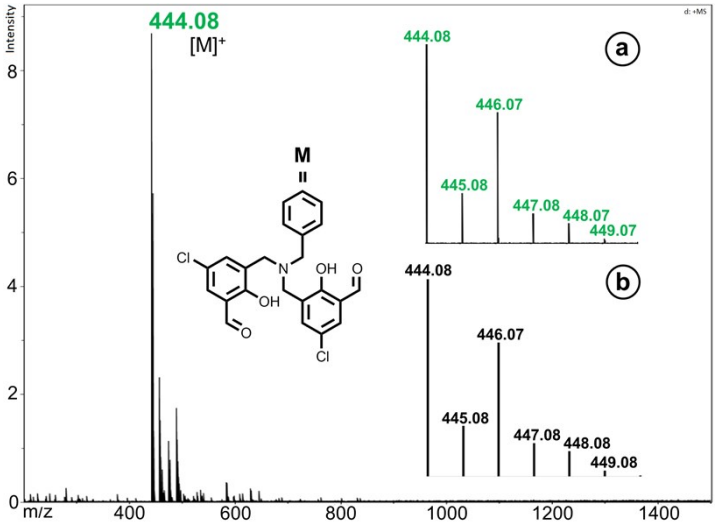


**Fig. S4** ESI-MS (positive) of $H_2Q_j$ in $CH_3OH$ together with inserted experimental (**a**) and simulative (**b**, calculation for $[C_{23}H_{19}Cl_2NO_4]$) peaks of isotopic distribution corresponding to the peak at m/z = 444.08.

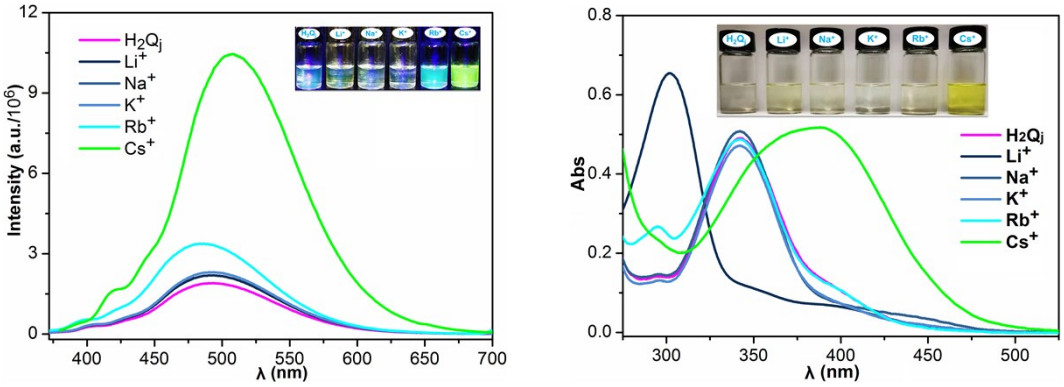


……**a**……**b**……

**Fig. S5** The fluorescence (**a**) and absorption (**b**) spectra of compound $H_2Q_j$ ([M] = 50 μM) with excessive alkali metal ions ([M] = 5 mM) in $CH_3OH$ at room temperature.

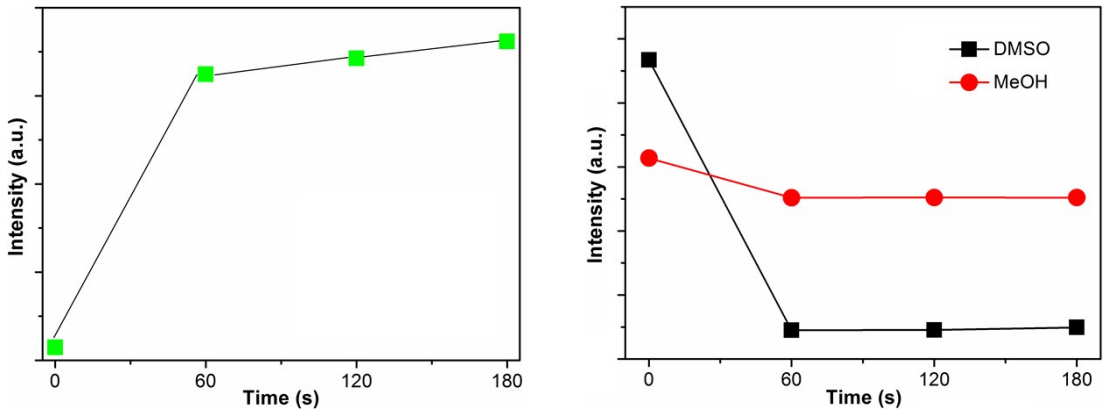


……**a**……**b**……

**Fig. S6** Time-dependent fluorescences ($\lambda_{em}$ = 507 nm) of $H_2Q_j$ with $Cs^+$ (**a**) and $CH_2Cl_2$ (**b**).

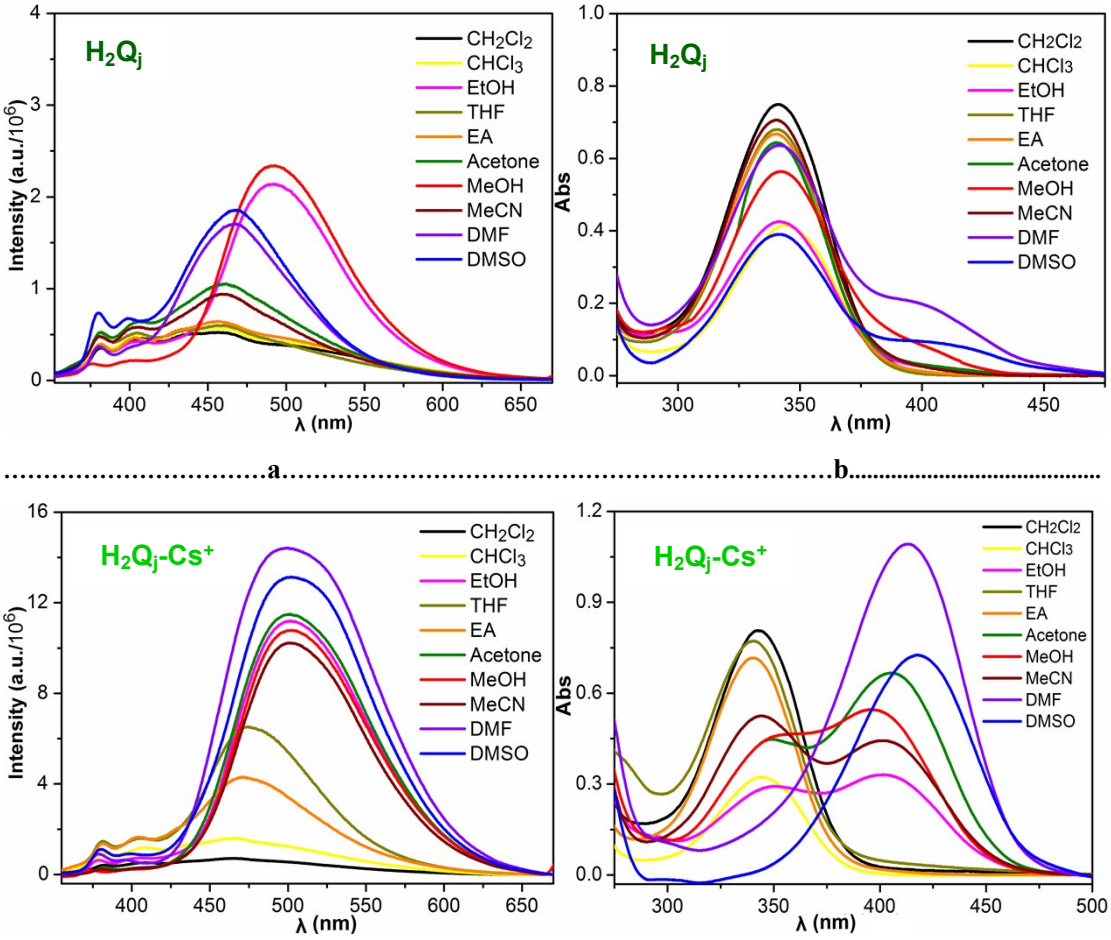


**Fig. S7** Fluorescence (**a** and **c**) and absorption (**b** and **d**) spectra for $H_2Q_j$ ([M] = 50 μM) and its $Cs^+$ mixture ($H_2Q_j$-$Cs^+$, [$H_2Q_j$] = 50 μM and [$Cs^+$] = 5 mM), respectively, in various solvents with 5% (*v*/*v*) $CH_3OH$ at the room temperature.

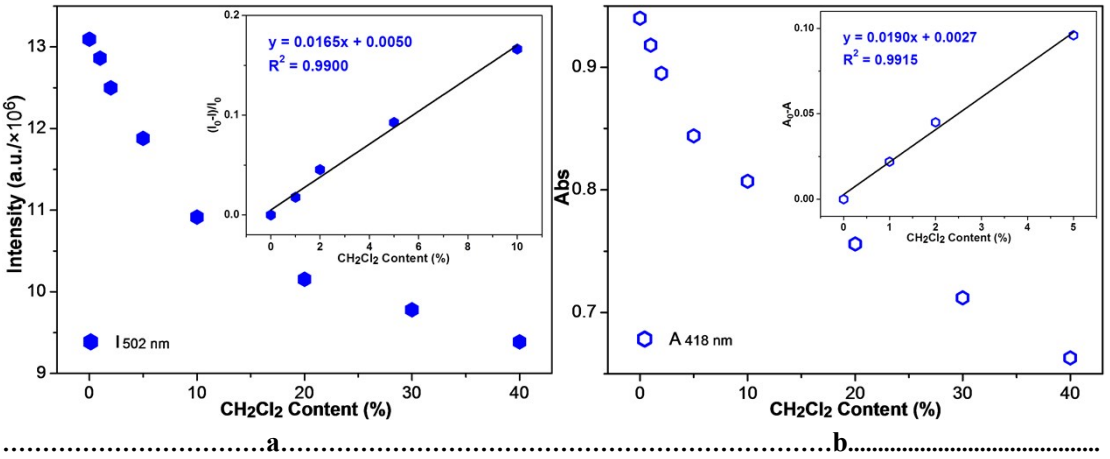

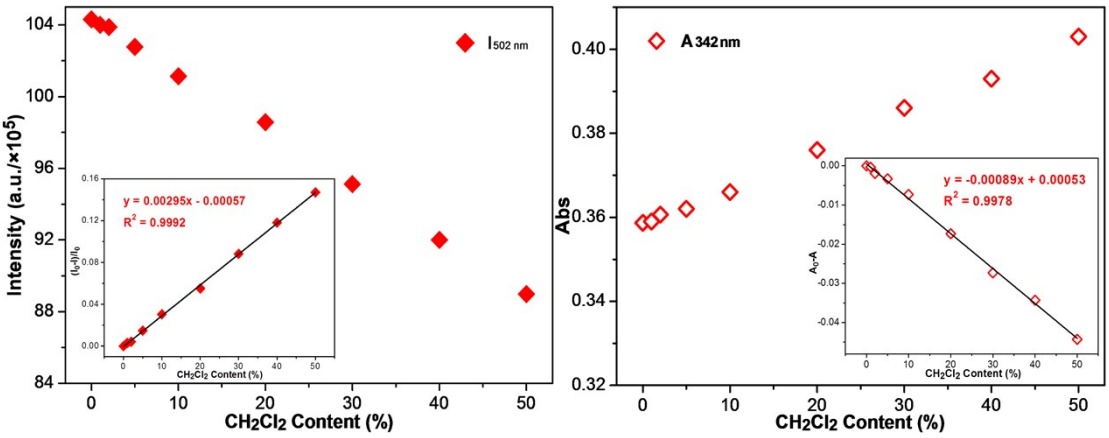


**……c……d……**

**Fig. S8** Changes of emission intensity ($\lambda_{em}$ = 502 nm) in DMSO (**a**) and $CH_3OH$ (**c**) with inserted linear calibration curve between the $(I_0\text{-}I)/I_0$ and $CH_2Cl_2$ content. Absorption variations and the plot of $(A_0\text{-}A)$ vs $CH_2Cl_2$ content at 418 nm (**b**) in DMSO and 342 nm (**d**) in $CH_3OH$.

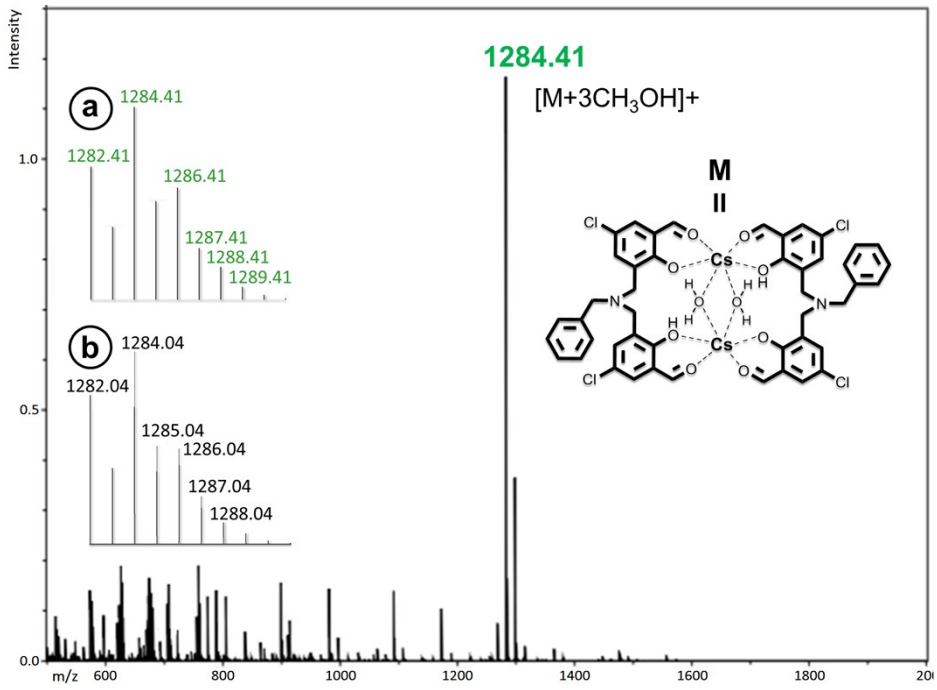


**Fig. S9** The ESI-MS (positive) of $H_2Q_j$ with excessive $Cs^+$ in $CH_3OH$ together with the inserted experimental (**a**) and simulative (**b**, calculation for $[C_{49}H_{51}Cl_4N_2O_{13}Cs_2]$) peaks of isotopic distribution corresponding to the peak at m/z = 1284.41.

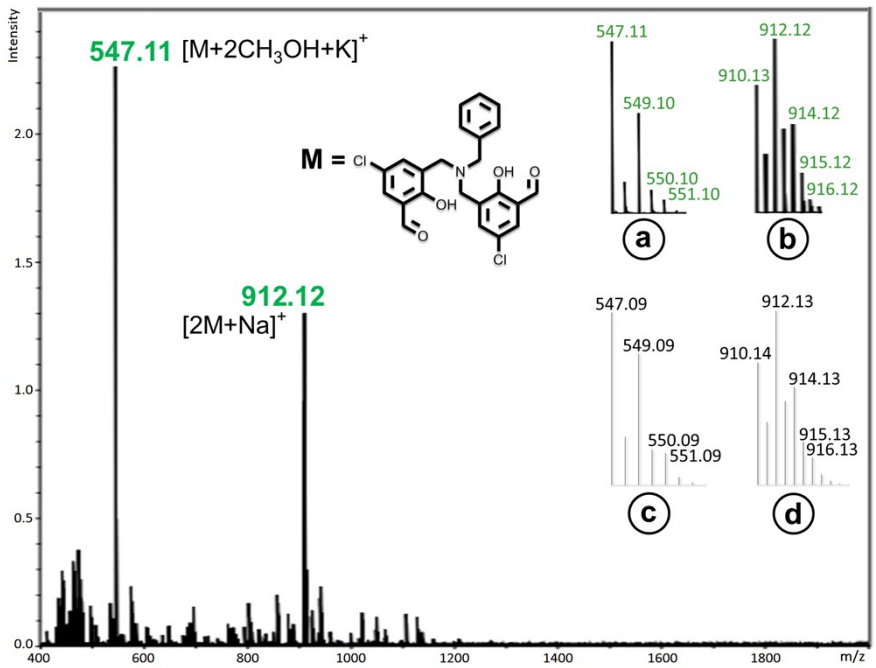


**Fig. S10** The ESI-MS (positive) of $H_2Q_j$ with excessive $Cs^+$ in $CH_3OH$-$CH_2Cl_2$ (*v*/*v* = 1:1) together with the inserted experimental (**a** and **b**) and simulative (**c** and **d**, calculation for $[C_{25}H_{27}Cl_2NO_6K]$ and $[C_{46}H_{38}Cl_4N_2O_8Na]$, respectively) peaks of isotopic distribution corresponding to the peaks at m/z = 547.11 and 912.12.

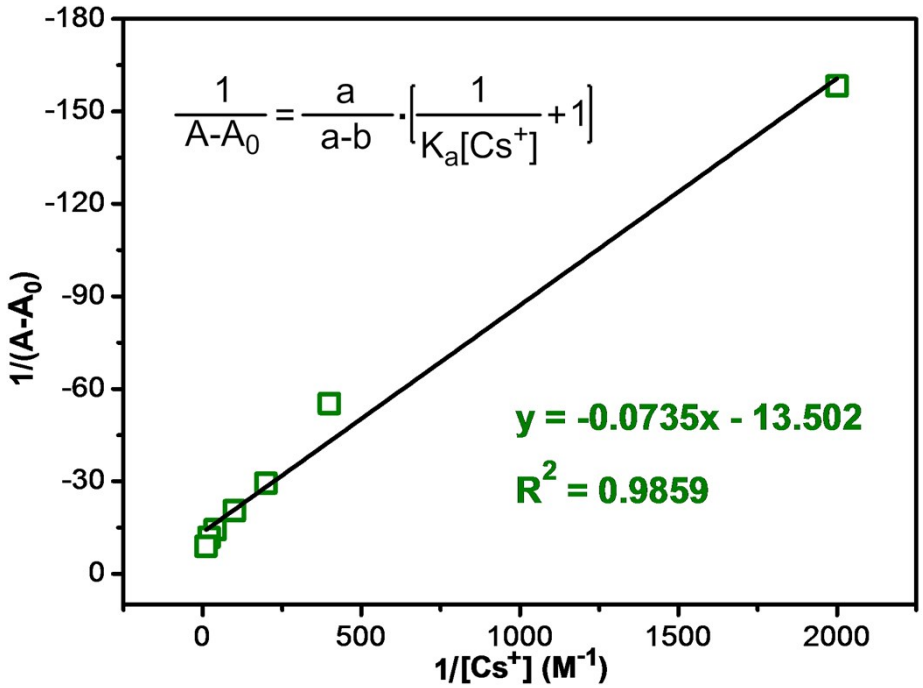


**Fig. S11** Benesi-Hildebrand analysis of sensor $H_2Q_j$ at different $Cs^+$ concentrations (0.50–100.0 M).

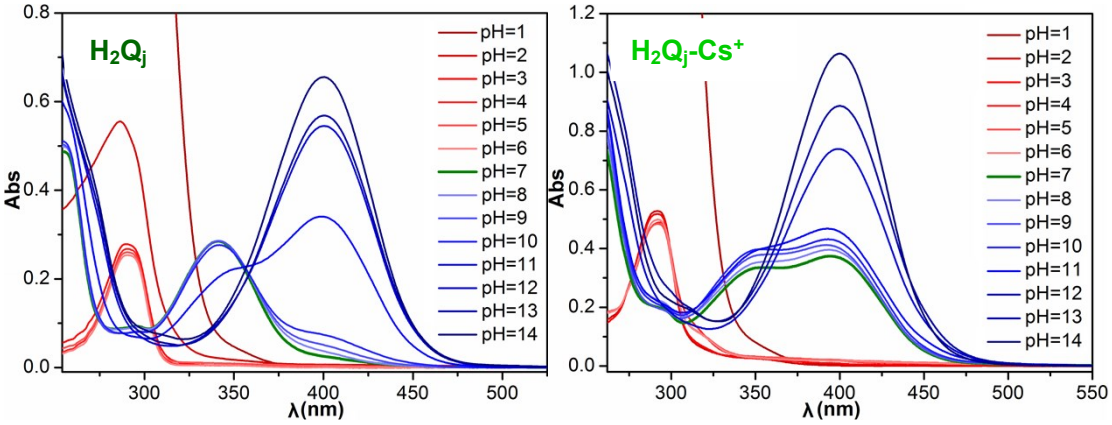


……**a**……**b**……

**Fig. S12** The absorption spectra of $H_2Q_j$ (**a**) ([M] = 100 μM) and $H_2Q_j$-$Cs^+$ mixture (**b**) ([$H_2Q_j$] = 100 μM and [$Cs^+$] = 100 mM) under different pH values (pH = 1−14) in $CH_3OH$ at room temperature.